Molecules and Cells

The Danger-Associated Peptide PEP1 Directs Cellular Reprogramming in the Arabidopsis Root Vascular System

Souvik Dhar[1], Hyoujin Kim[1], Cécile Segonzac[2,3,4], and Ji-Young Lee[1,3,4,*]

[1]School of Biological Sciences, College of Natural Science, Seoul National University, Seoul 08826, Korea, [2]Department of Agriculture, Forestry and Bioresources, Seoul National University, Seoul 00826, Korea, [3]Plant Genomics and Breeding Institute, Seoul National University, Seoul 08826, Korea, [4]Plant Immunity Research Center, Seoul National University, Seoul 08826, Korea
*Correspondence: jl924@snu.ac.kr
https://doi.org/10.14348/molcells.2021.0203
www.molcells.org

When perceiving microbe-associated molecular patterns (MAMPs) or plant-derived damage-associated molecular patterns (DAMPs), plants alter their root growth and development by displaying a reduction in the root length and the formation of root hairs and lateral roots. The exogenous application of a MAMP peptide, flg22, was shown to affect root growth by suppressing meristem activity. In addition to MAMPs, the DAMP peptide PEP1 suppresses root growth while also promoting root hair formation. However, the question of whether and how these elicitor peptides affect the development of the vascular system in the root has not been explored. The cellular receptors of PEP1, *PEPR1* and *PEPR2* are highly expressed in the root vascular system, while the receptors of flg22 (*FLS2*) and elf18 (*EFR*) are not. Consistent with the expression patterns of PEP1 receptors, we found that exogenously applied PEP1 has a strong impact on the division of stele cells, leading to a reduction of these cells. We also observed the alteration in the number and organization of cells that differentiate into xylem vessels. These PEP1-mediated developmental changes appear to be linked to the blockage of symplastic connections triggered by PEP1. PEP1 dramatically disrupts the symplastic movement of free green fluorescence protein (GFP) from phloem sieve elements to neighboring cells in the root meristem, leading to the deposition of a high level of callose between cells. Taken together, our first survey of PEP1-mediated vascular tissue development provides new insights into the PEP1 function as a regulator of cellular reprogramming in the Arabidopsis root vascular system.

Keywords: DAMP, MAMP, PEP1, root development, vascular system

INTRODUCTION

The plant root is an essential organ for the uptake of nutrients and water from the soil. Its growth is controlled by various endogenous and environmental factors. Among environmental factors, plant roots are exposed to an array of potential pathogenic organisms and adverse physical conditions, such as extreme temperatures, salinity, drought or heavy metals (De Coninck et al., 2015; Hacquard et al., 2017; Pascale et al., 2020). In particular, a root serves as the primary interface between a plant and soil microbes. Recent breakthroughs in root-microbiome interaction studies (Bartels et al., 2013; Emonet et al., 2021; Jing et al., 2019; Ma et al., 2014; Millet et al., 2010; Poncini et al., 2017; Zhou et al., 2020) suggest that upon the perception of microbe-associated molecular patterns (MAMP) or damage-associated molecular patterns

Received 30 July, 2021; revised 7 September, 2021; accepted 22 September, 2021; published online 12 November, 2021

eISSN: 0219-1032

(DAMP), the root epidermal layer transduces signals that trigger a burst of reactive oxygen species, elevating cytosolic calcium levels and activating defense-related genes and callose deposition processes. Unlike MAMPs, DAMPs such as plant elicitor peptides (PEPs) are produced and released by hosts in response to pathogenic organisms (Bartels and Boller, 2015). Thus far, eight genes have been identified in *Arabidopsis thaliana* (hereafter referred to as Arabidopsis) as those encoding PEP precursors (Bartels et al., 2013; Huffaker et al., 2006; Yamaguchi and Huffaker, 2011). Genes encoding the precursors of PEP1, 2, 3, and 8 are ubiquitously expressed in differentiated parts of a root, while genes for precursors of PEP4 and 7 are expressed in the root meristem (Bartels et al., 2013). A gene encoding a receptor for PEPs, *PEPR1*, is expressed in most tissue layers, whereas the expression of *PEPR2* is specific to the vascular cylinder (Bartels et al., 2013; Jing et al., 2019; Yamaguchi et al., 2010). Among the eight PEPs, PEP1 is a widely used elicitor in plant immunity research. Prolonged exposure to exogenous PEP1 plays a significant role not only in plant immunity but also in the regulation of root growth and root hair formation (Jing et al., 2019; Okada et al., 2021; Poncini et al., 2017; Yamaguchi et al., 2010; Zipfel et al., 2004). However, whether PEP1 affects the growth of the central vascular system and, if it does, how it occurs will require further studies.

The central vascular strand facilitates the long-distance transport of water, hormones, nutrients, proteins and other signaling molecules and provides mechanical support to vascular plants in terrestrial environments. In the root meristem, the vascular initials undergo a series of proliferative and formative cell divisions to establish themselves at the central part of the root, surrounded by the pericycle, endodermis, cortex and the outmost epidermal layer (De Rybel et al., 2016; Dolan et al., 1993; Seo et al., 2020). The quiescent center (QC) and neighboring stem cells constitute the stem cell niche, where cell lineages are established and maintained via formative divisions and where cell fate determination transpires (Aichinger et al., 2012; Sabatini et al., 2003; Wendrich et al., 2017). These complex developmental processes are extremely sensitive to signals sensing environmental changes (Chaiwanon et al., 2016; Perini et al., 2012). For instance, recent findings (Jang and Choi, 2018; Jang et al., 2017; Ramachandran et al., 2020; 2021) have revealed that xylem differentiation within the stele is largely influenced by reduced water availability via JA and ABA signaling.

Most studies of plant immunity have focused on pathogenic responses in leaves. One reason for this may be related to the rich information about pattern-recognition receptors (PRRs) in the shoot system (Beck et al., 2014). However, root-pathogen interaction studies have gained interest among researchers (Emonet et al., 2021; Jing et al., 2019; Okada et al., 2021; Poncini et al., 2017; Rich-Griffin et al., 2020; Zhou et al., 2020). Motivated by recent findings suggesting that a cocktail of MAMP (flg22) and DAMP (PEP1) can induce the expression of PRRs in the stele (Zhou et al., 2020), we wanted to know whether flg22 and elf18, among MAMP and PEP1 and among DAMP trigger any developmental changes within the stele in terms of cell division and differentiation.

To this end, we employed various phenotypic approaches to identify the developmental responses inside the root stele in Arabidopsis seedlings exposed to these elicitors during early growth. Intriguingly, our initial survey revealed that PEP1 can more potently control early vascular cell divisions within the stele as compared to flg22 and elf18. In accordance with this, we found that the expression of the PEP1 receptors of *PEPR1* and *PEPR2* are highly enriched within the stele, a probable cause of the magnitude of the responses triggered by PEP1. Furthermore, we observed that PEP1 stimulates ectopic xylem differentiation, leading to extra protoxylem or extra metaxylem in the root maturation zone. Finally, our work also revealed that PEP1 signaling may disrupt the symplastic connection through a phloem sieve element likely via callose deposition. Taken together, our results provide novel insights into the previously unknown function of PEP1 in controlling the developmental process of the Arabidopsis root stele.

MATERIALS AND METHODS

Plant materials and growth condition

The Arabidopsis plants used in this study were of the Columbia (Col-0) ecotype. Col-0 plants were used as the wild-type (WT) control in this study. The *fec* (*fls2 efr cerk1*) triple mutant (Gimenez-Ibanez et al., 2009), *ProWOX5:erGFP* (Sebastian et al., 2015); *ProTMO5::erGFP* (Lee et al., 2006); *ProARR5::erGFP* (Lee et al., 2006); *ProAHP6::erGFP* (Mähönen et al., 2006), *ProS32::erGFP* (Lee et al., 2006), *ProSUC2::GFP* (Imlau et al., 1999) and *ProTCSn::ntdTomato, ProDR5v2::n3GFP* (Smet et al., 2019) marker lines were reported previously. All seeds were surface-sterilized, vernalized and grown on half-MS media supplemented with 1% sucrose under a 16-h-light/8-h-dark cycle with light intensity of 100 μmol m^{-2} s^{-1} at 22°-23°C in a plant growth chamber.

Peptide biosynthesis

The peptides used in this study were synthesized by Peptron (Korea) (http://www.peptron.com). The sequences (from the N terminus to the C terminus) of the peptide used are as follows: flg22, TRLSSGLKINSAKDDAAGLQIA; elf18, Ac-SKEKFERTKPHVNVGTIG (Ac, acetyl group); and AtPEP1 (PEP1), ATKVKAKQRGKEKVSSGRPGHN. The peptides were dissolved in distilled water to make 10 mM of stock and were stored in a −20°C freezer until use.

Root growth inhibition assay with MAMP and DAMP treatments

To analyze root growth inhibition in the presence of MAMP (flg22 and elf18) or DAMP (PEP1) on solid half MS plates, seedlings grown on solid half MS plates were transferred two days after transfer (DAT) to a growth chamber onto fresh half MS plates supplemented with 1 μM of flg22 or 1 μM of elf18 or 1 μM of PEP1 or distilled water (mock). The seedlings were allowed to grow on the respective media for another five days. During this period, the seedlings were photographed every day.

To assess the degree of root growth inhibition in the liquid half MS media, three DAT seedlings were incubated in a six-well plate (SPL Life Sciences, Korea) with or without 1 μM

synthetic peptides (flg22, elf18, PEP1) for four days. During the treatment, the seedlings were arranged on a MS plate and photographed using a digital camera every day. The root lengths were measured by NIH Image J software (http://rsb.info.nih.gov/ij) as previously described (Okada et al., 2021).

Analysis of the stele cell number and xylem phenotype

To analyze the stele cell number and xylem phenotype in the MAMP or DAMP treated condition, seven DAT (upon a five-day treatment in respective media) seedling roots were harvested and fixed overnight in 4% paraformaldehyde at room temperature. The samples were then dehydrated in an ethanol series (30%, 50%, 70%, 90%, and 100% (v/v)) and plastic blocks were then prepared with Technovit 8100 kits according to the manufacturer's instructions. Plastic sections (5 μm width) were made using a Leica RM2255 microtome as described previously (Kim et al., 2020).

To determine the stele cell number, sections were prepared at the 1-1.5 mm basal region from the root tip. To determine the xylem phenotype, the 4-6 mm basal region from the root tip was used for sectioning. The sections were imaged using a Nikon Eclipse N*i*-U microscope with DIC optics.

Confocal microscopy

Confocal microscopy was performed on a Zeiss LSM700 and a Leica TCS SP8 confocal laser scanning microscope as previously reported (Kim et al., 2020; Seo and Lee, 2021). Pictures were taken with either a 20× dry objective lens or a 63× water-immersion objective lens. For Z-scan imaging, the same position on the root and the same laser scanning area were chosen.

To image the *ProTCSn::ntdTomato, ProDR5v2::n3GFP* dual-marker line, seedlings were fixed in 4% paraformaldehyde and treated with ClearSee solution (Kurihara et al., 2015) for five days. The seedlings were then stained with 0.1% (v/v) calcofluor white 2MR (Sigma-Aldrich, USA) in ClearSee solution for 30 min and observed under a confocal microscope (Leica TCS SP8) with preset excitation/emission wavelengths of 488 nm/500-530 nm for GFP, 550 nm/580 nm for tdTomato and 350 nm/420 nm for calcofluor white 2MR. To visualize the GFP protein in other transgenic lines, seedlings were stained in a 1 μM propidium iodide (PI; Sigma-Aldrich, USA) solution for 2 min and observed under a Carl Zeiss LSM700 confocal microscope (Carl Zeiss, Germany) with the following excitation and detection windows: GFP 488 nm/500-530 nm; PI 555 nm/591-635 nm.

Quantitative real-time polymerase chain reaction

Quantitative real-time polymerase chain reaction (qRT-PCR) assessments were carried out to analyze the relative transcript levels of the *PEPR1*, *PEPR2*, *ACS6*, *MYB51*, *WRKY11*, *ZAT12*, and *PER5* genes following a treatment with 1 μM of PEP1. To prepare the sample, five DAT seedlings grown on half MS plates were incubated in liquid half MS with or without 1 μM PEP1 for 6 h. After treatment, amounts of approximately 100 mg of root tissues were harvested per biological replicate and snap-frozen in liquid nitrogen. Total RNA was extracted using RNeasy plant mini kits (Qiagen, Germany) according to the manufacturer's instructions. The quality and quantity of the isolated RNA samples were analyzed by Nanodrop™ spectrophotometry (GE Healthcare, USA). Approximately 2 μg of purified RNA was used as a template for cDNA biosynthesis using SuperScript™ III Reverse Transcriptase (Invitrogen, USA) in 20 μl reaction amounts. The synthesized cDNA was diluted five-fold with autoclaved distilled H_2O, and 1 μl of c-DNA was used as a template for qRT-PCR using iQ™ SYBR® Green Supermix (Bio-Rad, USA) on a CFX96™ Real-Time PCR machine (Bio-Rad) following the manufacturer's instructions, as previously reported (Kim et al., 2020). The sequence information of the gene-specific primers is listed in Supplementary Table S1.

Callose deposition assay with aniline blue staining

To observe the callose deposition, four DAT transgenic seedlings of *ProS32::erGFP* (Lee et al., 2006) grown on half MS plates were transferred to other half-MS plates supplemented with 1 μM of PEP1 for two days. Mock- and PEP1-treated seedlings were fixed in 4% paraformaldehyde in 1× phosphate-buffered saline (PBS) (137 mM NaCl, 2.7 mM KCl, 10 mM Na_2HPO_4, 1.8 mM KH_2PO_4; pH 7.4) for an hour and washed three times in 1× PBS before they were rinsed with 1 ml of 67 mM K_2HPO_4 (1551128; Sigma-Aldrich). The root samples were then stained in 0.01% aniline blue (Sigma-Aldrich) dissolved in 67 mM K_2HPO_4 (pH 12) for 30-60 min at room temperature in the dark. Confocal images were obtained using a Leica TCS SP8 confocal microscope with preset excitation/emission wavelengths of 390 nm/420 nm for callose detection and 488 nm/500-530 nm for the GFP signals.

Accession numbers

The sequence information of the genes used in this study can be found in the Arabidopsis Genome Initiative under the following accession numbers: PEPR1 (AT1G73080); PEPR2 (AT1G17750); PER5 (AT1G14550); ACS6 (AT4G11280); MYB51 (AT1G18570); WRKY11 (AT4G31550); ZAT12 (AT5G59820); GAPDH (AT1G13440).

RESULTS

PEP1 inhibits the apical root growth without affecting the QC identity

The involvement of flg22, elf18, and PEP1 during the process of vascular cell division is currently unknown. Root growth inhibition caused by the prolonged exposure of seedlings to flg22, elf18, or PEP1 peptides has mostly been reported in liquid culture systems (Okada et al., 2021). However, to test the effects of these peptides on early root vascular development, we deemed it to be more appropriate to observe seedlings growing on a solid medium. In a root growth inhibition assay on solid half MS plates supplemented with 1 μM of flg22, elf18, and PEP1 (Figs. 1A-1C), PEP1 was the most potent peptide, retarding the root growth of two DAT seedlings from the initiation of the treatment. Compared to the mock condition (solid half MS media without any MAMP or DAMP), 1 μM of flg22 or elf18 only caused a marginal reduction of root growth (Figs. 1A and 1B).

To confirm the functionality of our flg22 or elf18 peptides, we monitored the root growth of Col-0 seedlings in liquid

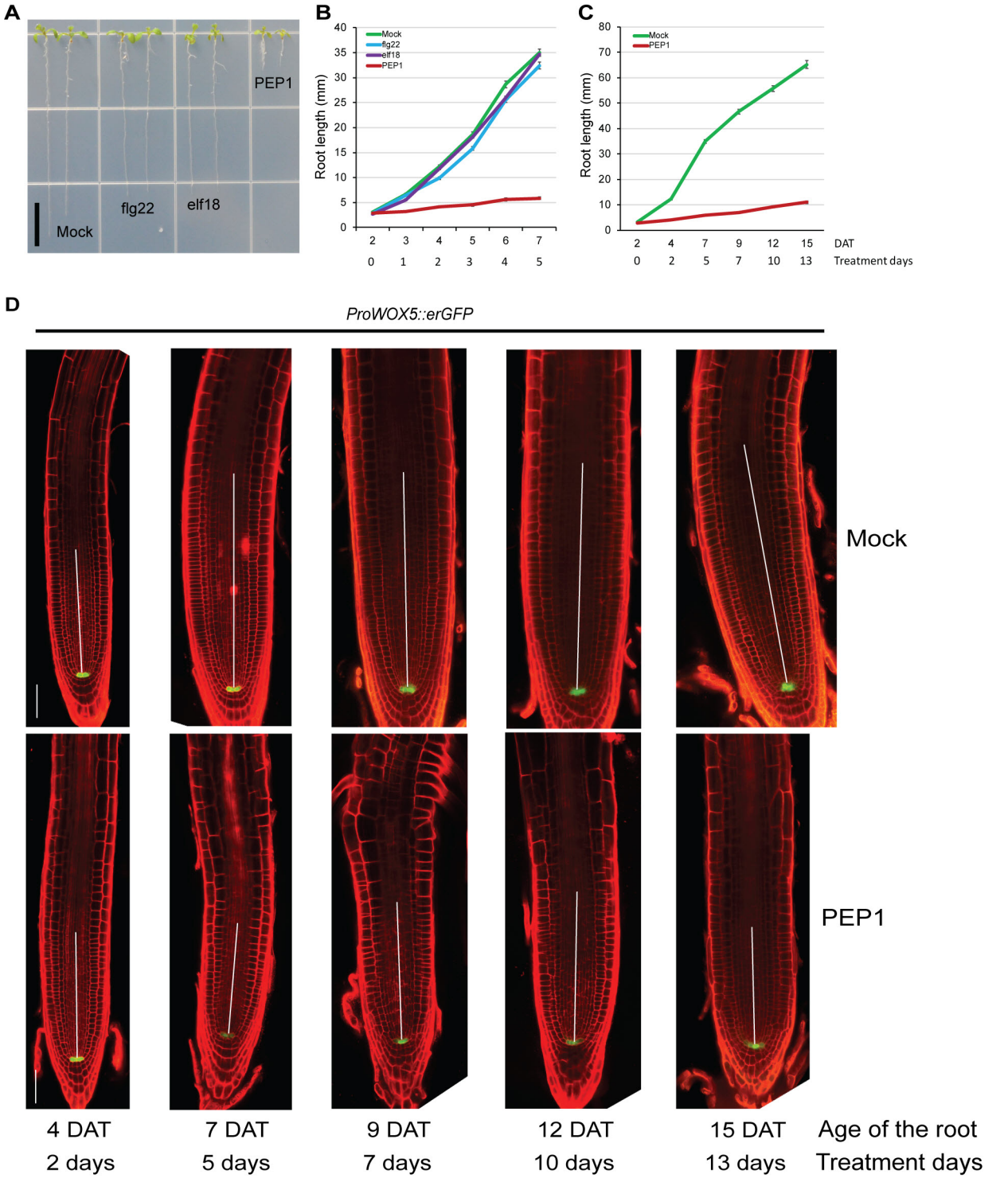

Fig. 1. Inhibition of the root growth by PEP1. (A) Two DAT Col-0 seedlings grown on half-MS agar plates containing 1 μM of flg22, elf18, or PEP1 or without elicitor for five days. Scale bar = 1 cm. (B) Root length of the two DAT seedlings grown on half-MS agar plates with or without an elicitor treatment. The length was measured in each consecutive day until five days. The data are shown as the mean ± SEM (n = 27-44 for each time point). (C) Root growth of two DAT WT seedlings grown on half-MS agar plates in the presence of 1 μM PEP1 at different time points. The data are shown as the mean ± SEM (n = 28-44 for each time point). (D) Microscopic analysis of *ProWOX5::erGFP* seedlings grown on PEP1 (1 μM) on half-MS agar plates at different time points. The white bar over the roots indicates the meristem regions. Scale bars = 50 μm.

half MS media containing 1 μM of flg22, elf18, and PEP1 (Supplementary Fig. S1A). Consistent with other findings (Okada et al., 2021), we observed strong suppression of root growth in liquid half MS media containing 1 μM of flg22 or elf18 (Supplementary Fig. S1B). Interestingly, PEP1 consistently suppressed root growth irrespective of the growth conditions. Moreover, the *fls2 efr cerk1* (*fec*) triple-receptor mutant (Gimenez-Ibanez et al., 2009), used as our experimental control for the flg22 and elf18 treatments, grew well when exposed to 1 μM of flg22 or elf18 (Supplementary Figs. S1C and S1D). As expected, the *fec* triple mutant showed a root growth inhibition phenotype similar to that of the Col-0 seedlings in the presence of 1 μM of PEP1 (Supplementary Fig. S1D). Therefore, our analysis indicates that the presence of PEP1 altered root growth irrespective of the media conditions, whereas flg22 or elf18 affected root growth mostly in the liquid culture system.

The QC plays a role in maintaining a stem cell population near the apical meristem that contributes to the addition of new cells to the developing root (Aida et al., 2004; Dolan et al., 1993; Scheres, 2007). We sought to determine whether the QC identity is affected by a long-term PEP1 treatment by monitoring the expression of *ProWOX5::erGFP* (Sarkar et al., 2007), a QC-specific marker. We treated two DAT seedlings harboring the *ProWOX5::erGFP* transgene with 1 μM of PEP1 and imaged them on 2, 5, 7, 10, and 13 days post treatment (Fig. 1D). Similar to mock-treated roots, *ProWOX5::erGFP* expression was retained in the QC for up to 13 days of the PEP1 treatment. Consistent with previous findings (Jing et al., 2019; Okada et al., 2021), our analysis suggests that PEP1 suppressed the root meristem activities without affecting the QC identity.

PEP1 signaling components are highly expressed in the root stele

Plasma-membrane-localized receptors play an essential role in recognizing the features of defense elicitors. This perception determines the magnitude of the plant immune responses (Abdul Malik et al., 2020; Nürnberger and Kemmerling, 2018). To understand the primary location at which these receptors perceive pathogenic signals, we examined the expression patterns of the receptors of flg22 (*FLS2*), elf18 (*EFR*), and PEP1 (*PEPR1* and *PEPR2*) peptides. In our cell-type-specific transcriptome data (Zhang et al., 2019), the receptors for PEP1 (*PEPR1* and *PEPR2*) are highly expressed in the stele compared to the other cell layers of the root, whereas *EFR* and *FLS2* maintained low expression levels in most tissue layers (Fig. 2A, Supplementary Table S2).

Next, we monitored the expression changes of two PEP1 receptors (*PEPR1* and *PEPR2*) and downstream-defense-associated marker genes, in this case *ACS6*, *MYB51*, *WRKY11*, *ZAT12*, and *PER5* (Poncini et al., 2017). The expression domains of the *PEPR* receptors are overlapped within the root stele (Bartels et al., 2013; Jing et al., 2019; Yamaguchi et al., 2010), whereas the expression levels of the defense-associated marker genes are largely induced in the root stele and the adjacent tissue layers upon the induction of biotic stress (Poncini et al., 2017). We extracted the expression dynamics of the PEP1 receptors and the downstream marker genes from a genome-wide expression dataset made available in a recent report (Bjornson et al., 2021). The transcriptions of these seven genes were clearly induced by treatments with flg22, elf18, and Pep1, an outcome not observed in the respective receptor mutants (Supplementary Table S3). To reconfirm whether the PEP1 treatment in our system could induce the expression of PEP1 receptors and the downstream-defense-associated marker genes, we monitored the expression changes of the seven genes (Supplementary Table S1) in the root after exposure to 1 μM of PEP1 for six hours by means of qRT-PCR (Figs. 2B-2H, Supplementary Fig. S2). The mRNA accumulations of *PEPR1* and *PEPR2* in the roots were strongly elevated after the PEP1 treatment (Figs. 2B and 2C, Supplementary Fig. S2), consistent with previous findings (Bjornson et al., 2021; Jing et al., 2019; Yamaguchi et al., 2010). Moreover, we confirmed the upregulation of the downstream marker genes (Figs. 2D-2H, Supplementary Fig. S2), indicating that in our conditions, the PEP1 treatment could effectively elicit defense responses in the roots. Taken together, these results suggest that PEP1 signaling exists within the stele, which may be predominant compared to flg22 and elf18.

PEP1 reduces the number of stele cells

The PEP1 coordination mechanisms of root apical growth and root hair development have recently been elucidated (Jing et al., 2019; Okada et al., 2021; Poncini et al., 2017). However, how these are related to the stele has not been reported. Therefore, we investigated whether PEP1 plays a role in the regulation of vascular tissue development. First, to test for an effect of PEP1 on the stele cell number, we quantified the stele cell number from the early elongation zone of the root. The stele cell file number enters a stable condition without further periclinal division as the cells exit the meristem region (Ye et al., 2021). Keeping this in mind, we undertook plastic sectioning at the transition zone of seven DAT roots that grew for five days in the presence of 1 μM of PEP1 (Figs. 3A and 3B). In the mock-treated samples, the stele cell number was approximately 49 ± 2 (Figs. 3A and 3E). Compared to the mock condition, the PEP1-treated sample showed a slight but significant ($P < 0.01$) reduction in the stele cell number (46 ± 2, Figs. 3B and 3E). However, consistent with the root growth suppression phenotype (Figs. 1A and 1B), treatment with 1 μM of flg22 and elf18 did not result in any noticeable change in the stele cell number compared to the mock condition (flg22 49 ± 1, elf18 50 ± 2, Figs. 3C-3E). These results suggest that PEP1 negatively affected stele cell formation in the root meristem.

PEP1 promotes extra xylem formation

Our finding that the stele cell number is reduced in the presence of PEP1 (Fig. 3), motivated a deeper investigation of xylem formation in response to PEP1. To analyze the organization of xylem vessels in a quantitative manner, we created cross-sections at the root differentiation zone of Col-0 seedlings treated with (PEP1) or without (mock) 1μM of PEP1 (Fig. 4). Based on the section images, we categorized vessel organizations into four types, as reported previously (Seo and Lee, 2021). The first type is defined as “five xylem cells” with

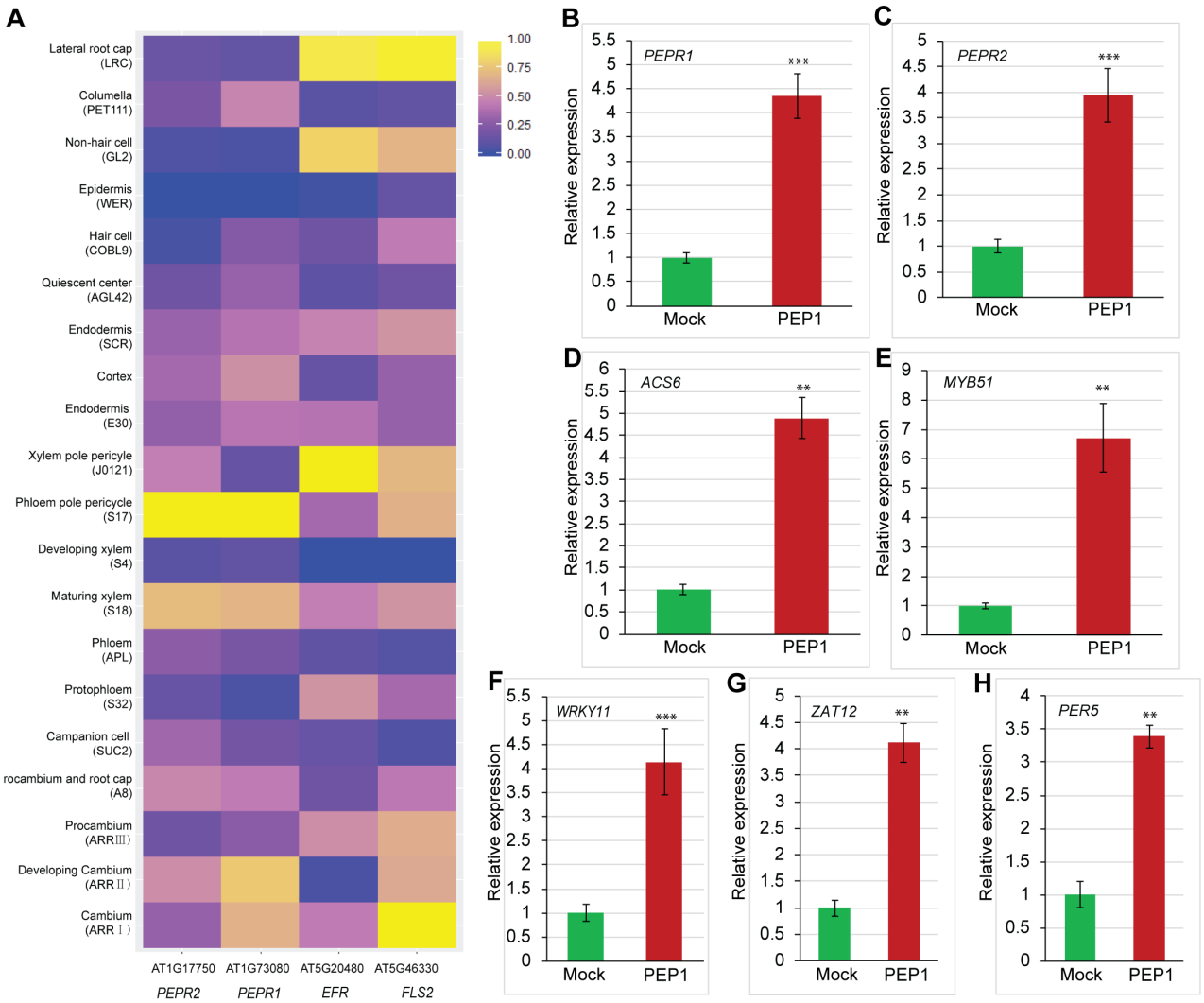

Fig. 2. Expression analysis of pathogenesis-related genes in response to PEP1. (A) Heat-map showing relative expression patterns of *PEPR1*, *PEPR2*, *EFR*, and *FLS2* receptors in the cell-type-specific expression data. The PEP1 receptors *PEPR1* and *PEPR2* show relatively high enrichment levels in stele cell files compared to *EFR* and *FLS2* receptors. Expression values for each gene were row-normalized with the cell file types. The cell-type-specific expression data are presented in Supplementary Table S2. (B and C) The relative m-RNA levels of the *PEPR1* and *PEPR2* receptors after 6-h post induction with 1 μM PEP1. The expression level of the mock treatment was arbitrarily set to 1.0 and compared to that, relative normalized expression values of the target genes were determined with a PEP1 treatment. The data are represented as the mean ± SEM (n = three individual reactions). Asterisks indicate statistical significance of differences between the corresponding values of the mock and PEP1 treatment samples. ***$P < 0.001$ (Student's *t*-test). (D-H) Relative expression levels of *ACS6*, *MYB51*, *WRKY11*, *ZAT12*, and *PER5* pathogenesis-related genes with a 6-h 1 μM PEP1 treatment. The normalized transcript levels compared to the mock treatment are indicated (± SEM from three individual reactions). The statistical significance of differences was calculated using Student's *t*-test (**$P < 0.01$; ***$P < 0.001$).

two protoxylem cells on opposite ends along the xylem axis and three metaxylem cells between them (Figs. 4A and 4D). The second category is defined as "extra xylem" where differentiated extra protoxylem or extra metaxylem cells outside the xylem axis can be observed (Figs. 4B and 4E). The third group is termed "six xylem cells" along the xylem axis with an extra xylem in a row (Figs. 4C and 4F). The final category was only observed in PEP1-treated roots. We termed it "4 xylem cells," where the section contains only four xylem cells in the xylem axis even after the differentiation process is completed (Fig. 4G).

In our analysis with 40 individual seedlings grown on half MS, we found that the most prevalent type (~50%) of xylem is that with "5 xylem cells," followed by the "6 xylem cells" (~45%) and the "extra xylem" (~5%) types (Fig. 4H). In the PEP1-treated roots, approximately 58% were categorized as the "5 xylem cells" type while close to 10% belonged to the "6 xylem cells" type. In addition, the "4 xylem cells" and "extra

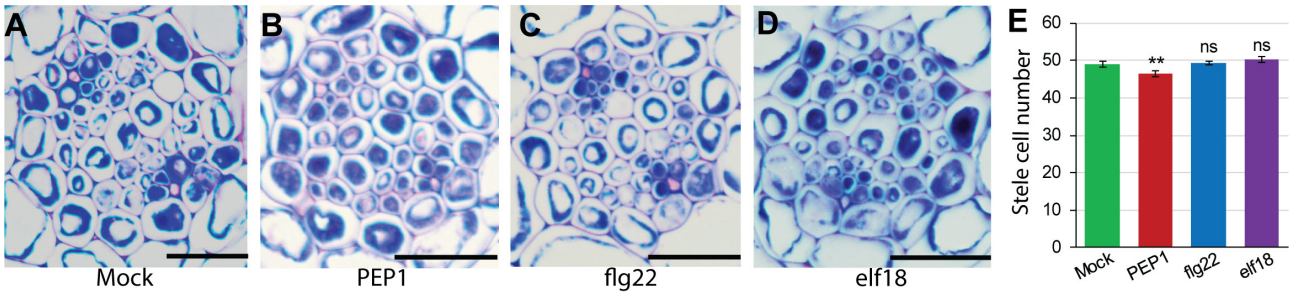

Fig. 3. Analysis of stele cell proliferation in response to PEP1. (A-D) Representative images of the cross-sections from the transition zones of roots treated for five days in 1 μM PEP1 (B) or flg22 (C), or elf18 (D). Roots without any elicitor treatments are denoted as mock (A). Scale bars = 12.5 μm. (E) Quantitative analysis of the stele cell file numbers from the cross-sections obtained through the transition zone. The data are shown as the mean ± SEM (n = 10). The statistical significance of differences was determined through Student's *t*-tests compared with the mock-treated sample. $**P < 0.01$; ns, not significant.

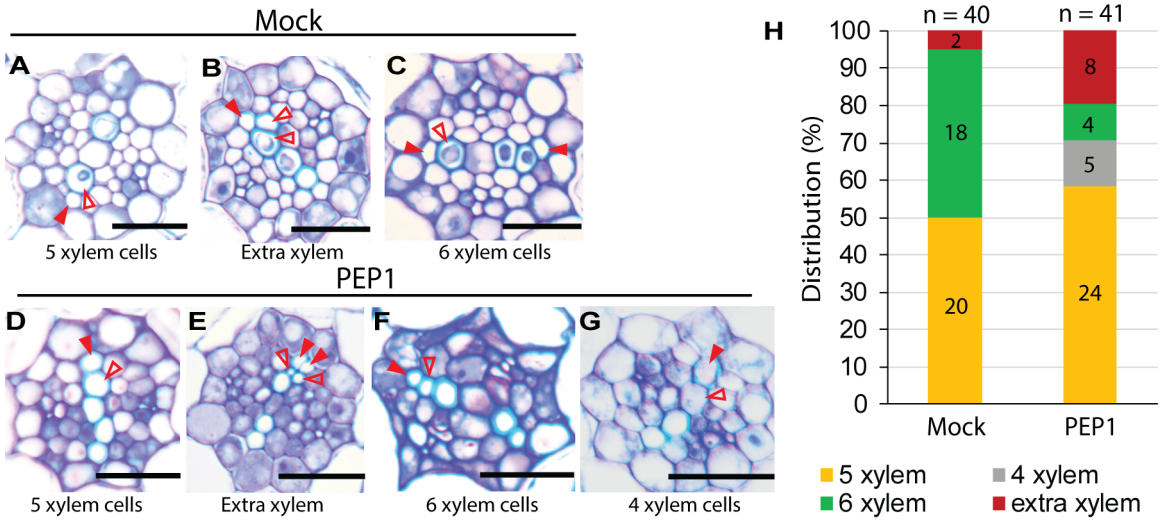

Fig. 4. Xylem organizations in PEP1 treated roots. (A-C) Representative images of three typical xylem arrangements in a mock-treated root sample. "5 xylem cells" phenotype (A), "extra xylem" phenotype (B), and "6 xylem cells" phenotype (C). Scale bars = 12.5 μm. (D-G) In the PEP1-treated sample, in addition to the "5 xylem cells" (D), "extra xylem" (E), and "6 xylem cells" (F) phenotypes, we identified a separate class of a "4 xylem cells" phenotype (G). Scale bars = 12.5 μm. (H) Quantification of the xylem phenotypes with a mock and a PEP1 treatment as categorized in (A-G). n = 40 (mock) and 41 (PEP1). Closed arrowheads, protoxylem; Open arrowheads, metaxylem.

xylem" types were found to account for approximately 12% and 20%, respectively (Fig. 4H). These data suggest that PEP1 modulates the xylem vessel number and distribution.

Xylem vessel fates in the root differentiation zone are determined early in xylem precursors in the root meristem (De Rybel et al., 2016). Thus, we selected cell-type-specific markers in the root meristem to cross-compare their expression responses to PEP1 and to assess changes in xylem vessel differentiation. Here, *ProTMO5::erGFP* (Lee et al., 2006) denotes the xylem axis (Fig. 5). We transferred four DAT *ProTMO5::erGFP* transgenic seedlings to half MS plates with or without 1 μM of PEP1 and incubated them for two days (Supplementary Fig. S3). Without PEP1, seedling roots grew 2.24 times (×2.24) on average in two days, while those treated with PEP1 grew only 1.29 times (×1.29) (Supplementary Fig. S3A). Consistent with these growth behaviors, the meristem size of the root treated with PEP1 became much smaller than that of mock-treated seedlings (Supplementary Figs. S3B and S3C). Under these conditions, the expression of *ProTMO5::erGFP* along the xylem axis of the meristem zone (Figs. 5A and 5E) could be divided into the "5 xylem cells" (Figs. 5B and 5F), "6 xylem cells" (Figs. 5C and 5G), and "extra xylem" (Figs. 5D and 5H) types. Our scoring of *ProTMO5::erGFP* revealed that the "extra xylem" frequency with the PEP1 treatment is elevated by twofold (~38%) in comparison with the mock-treated sample (~18%) (Fig. 5I). Moreover, there was a clear reduction of the "6 xylem cells" type (Mock: ~29%, PEP1: 15%), consistent with the scoring result of xylem vessels in the root differentiation zone (Figs. 4H and 5I).

We extended the xylem characterization further using lines expressing *ProAHP6::erGFP* (Mähönen et al., 2006) and

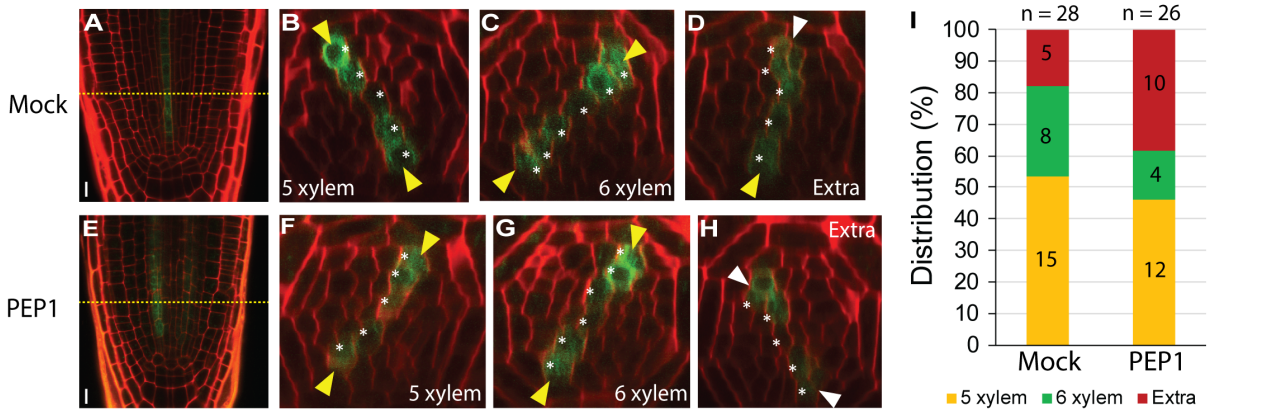

Fig. 5. Expression patterns of a xylem precursor specific marker under a PEP1 treatment. (A) Longitudinal image of *ProTMO5::erGFP* roots under 63X magnification. The yellow line in (A) represents the optical cross-section region shown in (B-D). Scale bar = 10 μm. (B-D) *TMO5* expression in the mock sample denotes three types of xylem organizations: the "5 xylem cells" (B), "6 xylem cells" (C), and "extra xylem" types (D). (E) Representative image of a *ProTMO5::erGFP* transgenic seedling treated with 1 μM of PEP1 for two days. The yellow line over the root meristem represents the region subjected to confocal Z-stack observations, as shown in (F-H). Scale bar = 10 μm. (F-H) The PEP1-treated roots were categorized into the "5 xylem cells" (F), "6 xylem cells" (G), and "extra xylem" (H) cell types depending on the *ProTMO5::erGFP* signal in the early vascular initials. The yellow arrowheads indicate the xylem axis, and the white arrowheads represent instances of extra cell division near the protoxylem ends. The white asterisks mark the xylem cell files in a row. (I) Quantification of the xylem morphology in mock-and PEP1-treated seedlings based on the *ProTMO5::erGFP* signals in the meristem.

ProARR5::erGFP (Lee et al., 2006) (Fig. 6). *ProAHP6::erGFP* is expressed in a protoxylem precursor and in the two neighboring pericycle cells (Figs. 6A-6H). In *ProAHP6::erGFP* seedlings, we found that nearly 42% of seedlings treated with PEP1 showed "lateral expansion" of the GFP signal near protoxylem precursor cells compared to only 24% of mock-treated seedlings (Fig. 6I). To reconfirm this "lateral expansion" of the protoxylem phenotype, we used *ProARR5::erGFP*, which specifically denotes the procambium tissue layers (Figs. 6J-6O). As expected, evidence of the expression of the *ProARR5::erGFP* marker was absent in the cells near the protoxylem precursor end ("retracted type") where *ProAHP6::erGFP* expression had expanded (Figs. 6D and 6H). We scored the *ProARR5::erGFP* expression pattern as the "normal type" when *ProARR5::erGFP* was expressed in all procambium tissue layers with one row of xylem cells between (~88% in mock- and ~50% in PEP1-treated seedlings, Figs. 6K, 6N, and 6P). We scored the *ProARR5::erGFP* expression pattern as the "retracted type," where the expression of *ProARR5::erGFP* was absent in cells neighboring the protoxylem precursor (~12% in mock- and ~50% in PEP1-treated seedlings, Figs. 6L, 6O, and 6P). These scoring results together with the xylem vessel organization analysis further corroborate our hypothesis that PEP1 modulates the boundaries between the procambium and xylem, resulting in the induction of the "extra xylem" phenotype.

Because auxin-cytokinin homeostasis also determines the boundaries between the procambium and xylem axis (Bishopp et al., 2011; De Rybel et al., 2016; Smetana et al., 2019), we sought to determine whether PEP1 regulates the auxin and cytokinin signaling domains in the root meristem. We used the dual-marker line expressing *ProTCSn::ntdTomato* and *ProDR5v2::n3GFP* (Smet et al., 2019) with 1 μM of PEP1 as a treatment for one day. The expression levels of *ProTCSn::ntdTomato* (*TCS*) and *ProDR5v2::n3GFP* (*DR5*) markers represent the cytokinin and auxin signaling domains, respectively. In the PEP1-treated seedlings, we could not find any significant differences in the signaling domains of auxin (*DR5*) and cytokinin (*TCS*) in the root meristem compared to mock-treated seedlings (Supplementary Fig. S4). Interestingly however, we observed a consistent decrease in the level of cytokinin signaling (*TCS*) in the columella stem cells of the PEP1-treated samples (Supplementary Figs. S4C and S4I).

PEP1 impairs symplastic movement in the *Arabidopsis* root meristem

The perception of MAMP or DAMP by their respective receptors induces callose deposition in the root elongation zone (Hou et al., 2014; Millet et al., 2010). We hypothesized that this phenomenon may disrupt the long-distance symplastic connections in the root. We therefore extended our study to examine whether PEP1 impairs long-distance transport via the phloem sieve element (SE). To address this, we performed two experiments. First, we visualized callose deposition in the root by aniline blue staining in seedlings harboring *ProS32::erGFP* (Lee et al., 2006) after two days of a PEP1 treatment (Figs. 7A and 7B). *S32* (AT2G18380) is specifically expressed in the phloem SEs, starting early in the root apical meristem (RAM) (Kim et al., 2020; Lee et al., 2006). In the mock condition, clear sieve plates were visible (Fig. 7A, marked by yellow arrows), whereas the roots treated with PEP1 showed evidence of the over-accumulation of callose on the sieve plate (Fig. 7B, marked with red arrows). Moreover, in contrast to earlier findings (Hou et al., 2014; Millet et al., 2010), we found callose deposition at the RAM only in PEP1-treated seedlings (Figs. 7A and 7B).

Subsequently, we investigated whether callose deposition in the presence of PEP1 could affect long-distance symplastic transport in the stele. To address this, we monitored the

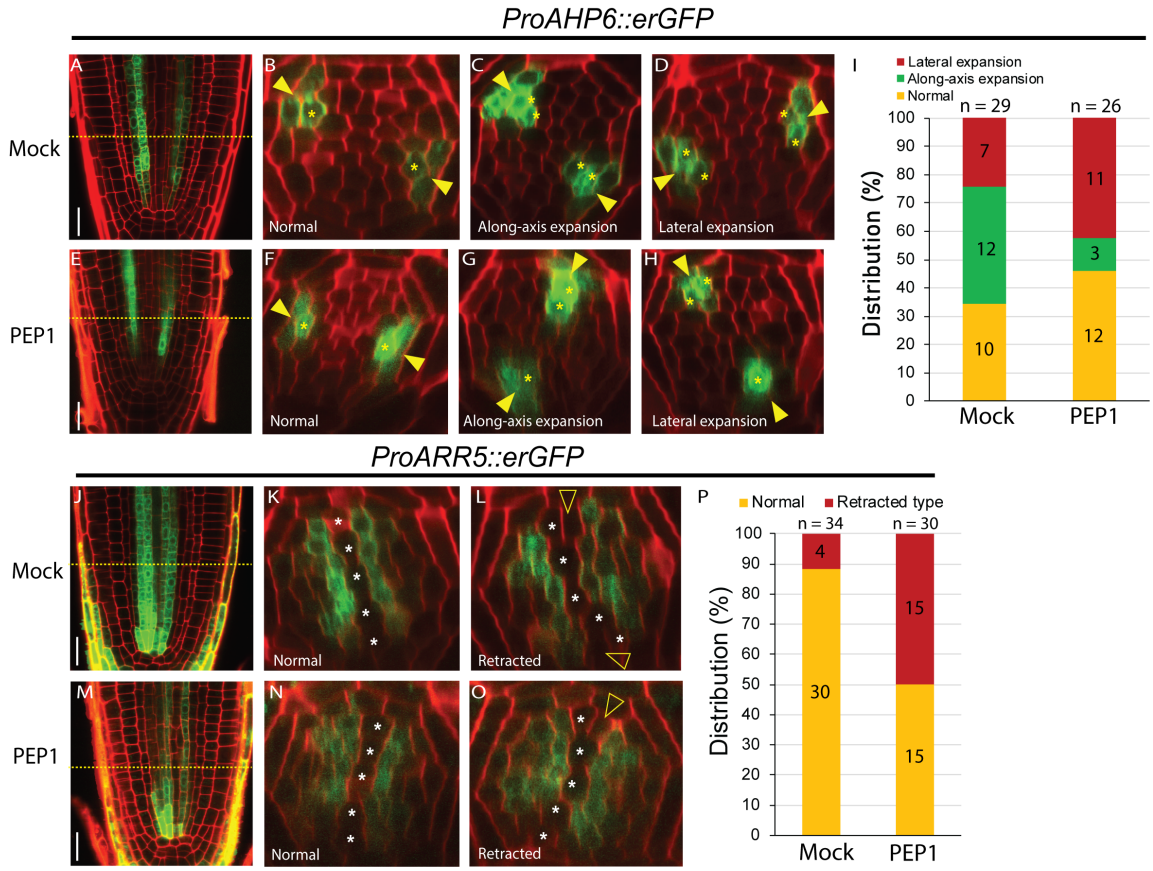

Fig. 6. Alterations in expression domains of *AHP6* and *ARR5* by PEP1. (A-D) Longitudinal (A) and cross-sectional (B-D) views of *ProAHP6::erGFP* transgenic seedlings after a mock treatment. The yellow line in (A) shows the region of the root where confocal Z-stack observations were made. (E-H) Expression pattern of *ProAHP6::erGFP* transgenic seedlings treated with 1 μM of PEP1 for two days. Based on the expression regions of *ProAHP6::erGFP*, we categorized the seedlings into three distinct classes: the "Normal" type, where *ProAHP6::erGFP* is expressed in one protoxylem initial with two neighboring pericycle cells; the "Along-axis expansion" type, where the expression domain of *AHP6* is expanded along the xylem axis towards the center; and the "lateral expansion" type, where *AHP6* is expressed in two neighboring cells in a side-by-side configuration near the protoxylem precursor end. The yellow arrowheads mark the xylem axis in the cross-section images. Yellow asterisks demarcate the cells where *AHP6* is expressed near the protoxylem precursor ends. Scale bars = 20 μm in (A and E). (I) Scoring results of mock- and PEP1-treated seedlings based on the *ProAHP6::erGFP* expression level in the early root meristem. (J-O) *ProARR5::erGFP* expression pattern in mock (J-L) and PEP1 (M-O) treated roots. The yellow line in (J and M) indicates the confocal Z-stack region. "Normal type" *ProARR5::erGFP* expression is limited to procambium cell files leaving a central row of xylem precursor cells (marked with white asterisks). "Retracted type" *ARR5* expression is absent in two or more cells near the protoxylem precursor ends. Open arrowheads indicate protoxylem cells where *ProARR5::erGFP* expressions are absent. Scale bars = 20 μm in (J and M). (P) Quantification result based on the *ProARR5::erGFP* expression domain in the mock- and PEP1-treated roots.

expression and transport patterns of free GFP molecules in *ProSUC2::GFP* seedlings. The *SUC2* promoter is specifically expressed in the companion cells (CCs) of the mature part of the root (Stadler and Sauer, 1996). In mock-treated seedlings, after its synthesis in the CCs of the root maturation zone, GFP was detected throughout the root, indicating that the free GFP protein migrated down through the phloem SEs to the root meristem and then moved in a cell-to-cell manner in the meristem region through the plasmodesmata (Fig. 7C). In contrast, in the PEP1-treated roots, the GFP signal was strictly retained in the phloem SE (Fig. 7C); accordingly, due to the over-accumulation of callose on the phloem sieve plate and plasmodesmata, the GFP molecules could not escape from the phloem. Taken together, these findings suggest that PEP1 disrupts the symplastic connections in the Arabidopsis root likely by triggering callose deposition on the sieve plates as well as the plasmodesmata between cells in the root meristem.

DISCUSSION

In this study, we uncovered novel regulatory roles of PEP1 in the root vasculature: i) PEP1, being derived from plants, reprograms the cellular machinery that is involved in the formative cell divisions within the stele; ii) PEP1 influences formation of ectopic proto-xylem and meta-xylem that modulate

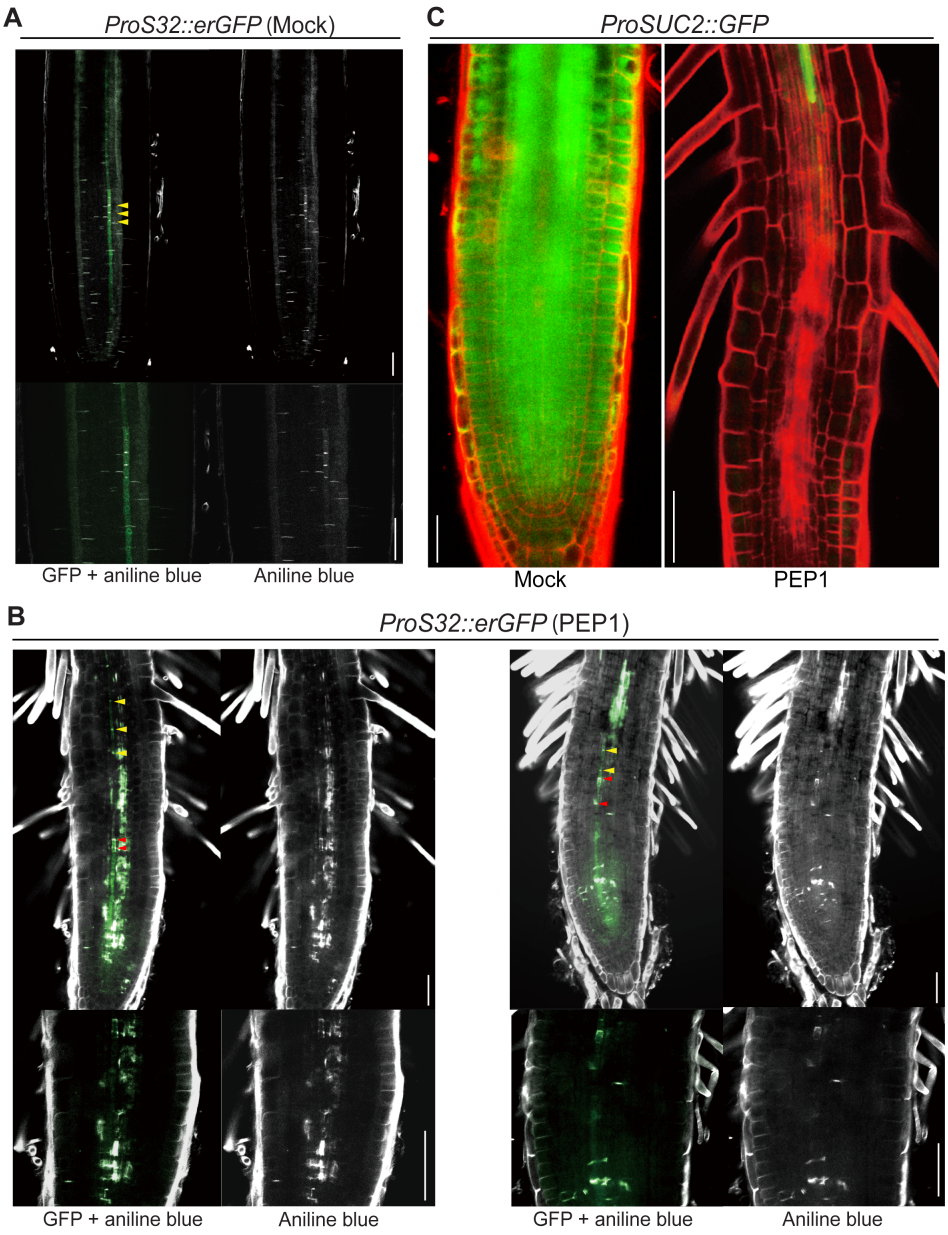

Fig. 7. Disruption in symplastic connections via PEP1 triggered-callose deposition. (A and B) aniline blue staining of WT seedlings treated with (B) or without (A) 1 μM of PEP1 for two days. Yellow arrowheads indicate the phloem sieve plates, whereas red arrowheads point to the callose-deposited sieve plates. Scale bars = 20 μm. (C) Root apical region of *ProSUC2::GFP* transgenic seedlings under a mock condition and with 1 μM of a PEP1 treatment for two days. Scale bars = 20 μm.

xylem-procambium boundaries; and iii) PEP1-induced callose deposition disrupts symplastic connections, thus affecting cell-to-cell communication in the root.

In addition to its role in plant immunity, an exogenous treatment of synthetic PEP1 controls cell division processes in the meristem, thereby affecting apical growth of the root (Jing et al., 2019; Okada et al., 2021). Most PEPs and PEP receptors (*PEPR*) are highly expressed in the root (Bartels et al., 2013). In an unperturbed condition, *PEPRs* are not expressed in the RAM, while exposure of the seedlings to synthetic PEP1 expands the expression domains of *PEPRs* to the meristem (Jing et al., 2019). Considering that the expression levels of *PEPs* and *PEPRs* are naturally enriched in vascular tissues, we cannot exclude the possibility that they are involved in the development of vascular tissue. How developmental changes are triggered by PEP pathways related to plant immunity should also be addressed.

In agreement with recent findings (Jing et al., 2019; Okada et al., 2021), we confirmed that PEP1 is the most potent elicitor peptide with regard to its ability to inhibit root growth compared to flg22 and elf18 (Figs. 1A-1C). The indeterminate growth of the root is supported by RAM, which is composed of a reservoir of undifferentiated cells that undergo formative and proliferative divisions, giving rise to a pool of daughter cells of correspondingly different and similar identities (Perini et al., 2012). In addition, it has been reported that at the early stages of root development, the meristem size rapidly increases until it reaches its final size at five days post germination (Perini et al., 2012). Keeping this in mind, we exposed early stages of the seedlings (2 DAT) to PEP1. In

mock-treated roots, the meristem size increased significantly at an early time point, whereas no such visible increase in the meristem size was observed in the roots treated with PEP1 (Fig. 1D). These results together with previous findings (Jing et al., 2019; Okada et al., 2021) suggest that PEP1-induced signaling exists in the RAM and actively inhibits proliferative cell divisions. Moreover, we observed that with a long-term PEP1 treatment, the cellular identity of the QC does not change (Fig. 1D). This finding indicates that root growth inhibited by PEP1 is not from the degeneration of the stem cell niche. Consistent with this, we observed root growth recovery when the seedlings were moved back to media without PEP1 (data not shown).

We then asked whether PEP1 affects the formative cell divisions in the root stele. To address this, we initially counted the stele cell file number from the transition zone of the root (Fig. 3). The cell file number reaches a stable condition at the transition zone without further formative divisions (Ye et al., 2021). Based on our analysis of the stele cell file number (Fig. 3E), it is tempting to speculate that in addition to the proliferative divisions in the RAM, PEP1 also controls formative divisions of the vascular initials. We then observed how the xylem vessel distribution is affected by PEP1. Our extensive phenotypic analyses with PEP1-treated roots (Fig. 4) revealed that PEP1 modifies the frequency and distribution of the xylem vessels. Compared to mock-treated roots, we found that there is an increase in ectopic "proto-xylem" and "meta-xylem" formation outcomes with the PEP1 treatment. Additionally, we observed there is a decrease in the number of xylem cells along the xylem axis upon exposure to PEP1. Intriguingly, the study with cell-type-specific markers (Figs. 5 and 6) further corroborates our xylem phenotype results obtained through a PEP1 treatment. These observations collectively strengthen our contention that PEP1-mediated molecular signaling acts strongly to reprogram the cellular machinery in the vascular initials and modifies the cellular boundaries between the xylem and procambium in the primary root.

Our finding leads to the question of how the formation of cellular boundaries is controlled by PEP1. It is well known that molecular cross-talk between auxin-cytokinin signaling maintains cellular homeostasis between the procambium and xylem (De Rybel et al., 2016). However, in our study involving a short-term PEP1 treatment, we could not find any significant alteration of auxin-cytokinin domains (Supplementary Fig. S4). We previously reported that AT-hook motif nuclear localized proteins (AHLs) tightly control the xylem-procambium boundaries (Seo and Lee, 2021; Zhou et al., 2013). However, it is not known whether AHL transcriptional networks are influenced by PEP1. Molecular-genetic studies are needed to determine whether this is the case in the future.

The exposure of the seedlings to defense elicitors causes callose deposition in the root (Hou et al., 2014; Millet et al., 2010). We monitored this aspect further in relation to the cell-to-cell communications via symplastic pathways. The symplastic transport process is mediated by plasmodesmata that integrates the local movement of molecules with long-distance transport through phloem loading and unloading (Sevilem et al., 2013). The phloem SE that plays a predominant role in long-distance transport is differentiated early in the root meristem (Kim et al., 2020; Seo et al., 2020). With the use of the phloem SE specific marker *ProS32::erGFP*, we observed that a PEP1 treatment causes callose deposition on the sieve plates, which may disrupt the long-distance transport process (Figs. 7A and 7B). Moreover, as a possible consequence of the altered callose deposition upon a PEP1 treatment, we did not observe any unloading of GFP molecules (derived from the *SUC2* promoter) into the cells of the root meristem (Fig. 7C). These findings further support the idea that PEP1 impairs long-distance transport and symplastic connections in the Arabidopsis root by clogging the plasmodesmatal channels with callose.

In summary, our findings have revealed novel roles of PEP1 in controlling vascular tissue differentiation and symplastic transport in the Arabidopsis root stele. This is the first detailed study that reports the dynamic influence of PEP1 on vascular tissue development. Future studies are needed to uncover the underlying molecular mechanisms and how these complex developmental responses triggered by PEP1 are related to plant immunity.

Note: Supplementary information is available on the Molecules and Cells website (www.molcells.org)

ACKNOWLEDGMENTS

We thank the members of the Lee lab for assisting in the experiments at various stages. This work was supported by the grants NRF-2018R1A5A1023599 to J.Y.L. and C.S. and NRF-2021R1A2C3006061 to J.Y.L. from National Research Foundation of Korea. S.D. was supported by the Brain Korea 21 Plus Program. H.K. was supported by WooDuk Foundation.

AUTHOR CONTRIBUTIONS

J.Y.L. conceived the project. S.D. and J.Y.L. designed the research. S.D. and H.K. performed experiments. S.D., H.K., and J.Y.L. analyzed and interpreted the data. S.D. wrote the first draft. S.D., C.S., and J.Y.L. corrected and finalized the manuscript. All authors have seen and approved the manuscript prior to submission.

CONFLICT OF INTEREST

The authors have no potential conflicts of interest to disclose.

ORCID

Souvik Dhar https://orcid.org/0000-0002-9693-8145
Hyoujin Kim https://orcid.org/0000-0003-3317-6996
Cécile Segonzac https://orcid.org/0000-0002-5537-7556
Ji-Young Lee https://orcid.org/0000-0002-7631-5127

REFERENCES

Abdul Malik, N.A., Kumar, I.S., and Nadarajah, K. (2020). Elicitor and receptor molecules: orchestrators of plant defense and immunity. Int. J. Mol. Sci. *21*, 963.

Aichinger, E., Kornet, N., Friedrich, T., and Laux, T. (2012). Plant stem cell niches. Annu. Rev. Plant Biol. *63*, 615-636.

Aida, M., Beis, D., Heidstra, R., Willemsen, V., Blilou, I., Galinha, C., Nussaume, L., Noh, Y.S., Amasino, R., and Scheres, B. (2004). The PLETHORA genes mediate patterning of the Arabidopsis root stem cell niche. Cell *119*, 109-120.

Bartels, S. and Boller, T. (2015). Quo vadis, Pep? Plant elicitor peptides at the crossroads of immunity, stress, and development. J. Exp. Bot. *66*, 5183-5193.

Bartels, S., Lori, M., Mbengue, M., van Verk, M., Klauser, D., Hander, T., Boni, R., Robatzek, S., and Boller, T. (2013). The family of Peps and their precursors in Arabidopsis: differential expression and localization but similar induction of pattern-triggered immune responses. J. Exp. Bot. *64*, 5309-5321.

Beck, M., Wyrsch, I., Strutt, J., Wimalasekera, R., Webb, A., Boller, T., and Robatzek, S. (2014). Expression patterns of FLAGELLIN SENSING 2 map to bacterial entry sites in plant shoots and roots. J. Exp. Bot. *65*, 6487-6498.

Bishopp, A., Help, H., El-Showk, S., Weijers, D., Scheres, B., Friml, J., Benkova, E., Mahonen, A.P., and Helariutta, Y. (2011). A mutually inhibitory interaction between auxin and cytokinin specifies vascular pattern in roots. Curr. Biol. *21*, 917-926.

Bjornson, M., Pimprikar, P., Nürnberger, T., and Zipfel, C. (2021). The transcriptional landscape of Arabidopsis thaliana pattern-triggered immunity. Nat. Plants *7*, 579-586.

Chaiwanon, J., Wang, W., Zhu, J.Y., Oh, E., and Wang, Z.Y. (2016). Information integration and communication in plant growth regulation. Cell *164*, 1257-1268.

De Coninck, B., Timmermans, P., Vos, C., Cammue, B.P.A., and Kazan, K. (2015). What lies beneath: belowground defense strategies in plants. Trends Plant Sci. *20*, 91-101.

De Rybel, B., Mahonen, A.P., Helariutta, Y., and Weijers, D. (2016). Plant vascular development: from early specification to differentiation. Nat. Rev. Mol. Cell Biol. *17*, 30-40.

Dolan, L., Janmaat, K., Willemsen, V., Linstead, P., Poethig, S., Roberts, K., and Scheres, B. (1993). Cellular organisation of the Arabidopsis thaliana root. Development *119*, 71-84.

Emonet, A., Zhou, F., Vacheron, J., Heiman, C.M., Tendon, V.D., Ma, K.W., Schulze-Lefert, P., Keel, C., and Geldner, N. (2021). Spatially restricted immune responses are required for maintaining root meristematic activity upon detection of bacteria. Curr. Biol. *31*, 1012-1028.e7.

Gimenez-Ibanez, S., Ntoukakis, V., and Rathjen, J.P. (2009). The LysM receptor kinase CERK1 mediates bacterial perception in Arabidopsis. Plant Signal. Behav. *4*, 539-541.

Hacquard, S., Spaepen, S., Garrido-Oter, R., and Schulze-Lefert, P. (2017). Interplay between innate immunity and the plant microbiota. Annu. Rev. Phytopathol. *55*, 565-589.

Hou, S., Wang, X., Chen, D., Yang, X., Wang, M., Turrà, D., Di Pietro, A., and Zhang, W. (2014). The secreted peptide PIP1 amplifies immunity through receptor-like kinase 7. PLoS Pathog. *10*, e1004331.

Huffaker, A., Pearce, G., and Ryan, C.A. (2006). An endogenous peptide signal in Arabidopsis activates components of the innate immune response. Proc. Natl. Acad. Sci. U. S. A. *103*, 10098-10103.

Imlau, A., Truernit, E., and Sauer, N. (1999). Cell-to-cell and long-distance trafficking of the green fluorescent protein in the phloem and symplastic unloading of the protein into sink tissues. Plant Cell *11*, 309-322.

Jang, G., Chang, S.H., Um, T.Y., Lee, S., Kim, J.K., and Choi, Y.D. (2017). Antagonistic interaction between jasmonic acid and cytokinin in xylem development. Sci. Rep. *7*, 10212.

Jang, G. and Choi, Y.D. (2018). Drought stress promotes xylem differentiation by modulating the interaction between cytokinin and jasmonic acid. Plant Signal. Behav. *13*, e1451707.

Jing, Y., Zheng, X., Zhang, D., Shen, N., Wang, Y., Yang, L., Fu, A., Shi, J., Zhao, F., Lan, W., et al. (2019). Danger-associated peptides interact with PIN-dependent local auxin distribution to inhibit root growth in Arabidopsis. Plant Cell *31*, 1767-1787.

Kim, H., Zhou, J., Kumar, D., Jang, G., Ryu, K.H., Sebastian, J., Miyashima, S., Helariutta, Y., and Lee, J.Y. (2020). SHORTROOT-mediated intercellular signals coordinate phloem development in Arabidopsis roots. Plant Cell *32*, 1519-1535.

Kurihara, D., Mizuta, Y., Sato, Y., and Higashiyama, T. (2015). ClearSee: a rapid optical clearing reagent for whole-plant fluorescence imaging. Development *142*, 4168-4179.

Lee, J.Y., Colinas, J., Wang, J.Y., Mace, D., Ohler, U., and Benfey, P.N. (2006). Transcriptional and posttranscriptional regulation of transcription factor expression in Arabidopsis roots. Proc. Natl. Acad. Sci. U. S. A. *103*, 6055-6060.

Ma, C., Guo, J., Kang, Y., Doman, K., Bryan, A.C., Tax, F.E., Yamaguchi, Y., and Qi, Z. (2014). AtPEPTIDE RECEPTOR2 mediates the AtPEPTIDE1-induced cytosolic Ca2+ rise, which is required for the suppression of Glutamine Dumper gene expression in Arabidopsis roots. J. Integr. Plant Biol. *56*, 684-694.

Mähönen, A.P., Bishopp, A., Higuchi, M., Nieminen, K.M., Kinoshita, K., Törmäkangas, K., Ikeda, Y., Oka, A., Kakimoto, T., and Helariutta, Y. (2006). Cytokinin signaling and its inhibitor AHP6 regulate cell fate during vascular development. Science *311*, 94-98.

Millet, Y.A., Danna, C.H., Clay, N.K., Songnuan, W., Simon, M.D., Werck-Reichhart, D., and Ausubel, F.M. (2010). Innate immune responses activated in Arabidopsis roots by microbe-associated molecular patterns. Plant Cell *22*, 973-990.

Nürnberger, T. and Kemmerling, B. (2018). Pathogen-associated molecular patterns (PAMP) and PAMP-triggered immunity. In Annual Plant Reviews Online, J.A. Roberts, ed. (Hoboken, NJ: John Wiley & Sons), https://doi.org/10.1002/9781119312994.apr0362

Okada, K., Kubota, Y., Hirase, T., Otani, K., Goh, T., Hiruma, K., and Saijo, Y. (2021). Uncoupling root hair formation and defence activation from growth inhibition in response to damage-associated Pep peptides in Arabidopsis thaliana. New Phytol. *229*, 2844-2858.

Pascale, A., Proietti, S., Pantelides, I.S., and Stringlis, I.A. (2020). Modulation of the root microbiome by plant molecules: the basis for targeted disease suppression and plant growth promotion. Front. Plant Sci. *10*, 1741.

Perini, S., Mambro, R., and Sabatini, S. (2012). Growth and development of the root apical meristem. Curr. Opin. Plant Biol. *15*, 17-23.

Poncini, L., Wyrsch, I., Dénervaud Tendon, V., Vorley, T., Boller, T., Geldner, N., Métraux, J.P., and Lehmann, S. (2017). In roots of Arabidopsis thaliana, the damage-associated molecular pattern AtPep1 is a stronger elicitor of immune signalling than flg22 or the chitin heptamer. PLoS One *12*, e0185808.

Ramachandran, P., Augstein, F., Mazumdar, S., Van Nguyen, T., Minina, E.A., Melnyk, C.W., and Carlsbecker, A. (2021). Abscisic acid signaling activates distinct VND transcription factors to promote xylem differentiation in Arabidopsis. Curr. Biol. *31*, 3153-3161.e5.

Ramachandran, P., Augstein, F., Nguyen, V., and Carlsbecker, A. (2020). Coping with water limitation: hormones that modify plant root xylem development. Front. Plant Sci. *11*, 570.

Rich-Griffin, C., Eichmann, R., Reitz, M.U., Hermann, S., Woolley-Allen, K., Brown, P.E., Wiwatdirekkul, K., Esteban, E., Pasha, A., Kogel, K.H., et al. (2020). Regulation of cell type-specific immunity networks in Arabidopsis roots. Plant Cell *32*, 2742-2762.

Sabatini, S., Heidstra, R., Wildwater, M., and Scheres, B. (2003). SCARECROW is involved in positioning the stem cell niche in the Arabidopsis root meristem. Genes Dev. *17*, 354-358.

Sarkar, A.K., Luijten, M., Miyashima, S., Lenhard, M., Hashimoto, T., Nakajima, K., Scheres, B., Heidstra, R., and Laux, T. (2007). Conserved factors regulate signalling in Arabidopsis thaliana shoot and root stem cell organizers. Nature *446*, 811-814.

Scheres, B. (2007). Stem-cell niches: nursery rhymes across kingdoms. Nat. Rev. Mol. Cell Biol. *8*, 345-354.

Sebastian, J., Ryu, K.H., Zhou, J., Tarkowská, D., Tarkowski, P., Cho, Y.H., Yoo,

S.D., Kim, E.S., and Lee, J.Y. (2015). PHABULOSA controls the quiescent center-independent root meristem activities in Arabidopsis thaliana. PLoS Genet. *11*, e1004973.

Seo, M., Kim, H., and Lee, J.Y. (2020). Information on the move: vascular tissue development in space and time during postembryonic root growth. Curr. Opin. Plant Biol. *57*, 110-117.

Seo, M. and Lee, J.Y. (2021). Dissection of functional modules of AT-HOOK MOTIF NUCLEAR LOCALIZED PROTEIN 4 in the development of the root xylem. Front. Plant Sci. *12*, 632078.

Sevilem, I., Miyashima, S., and Helariutta, Y. (2013). Cell-to-cell communication via plasmodesmata in vascular plants. Cell Adh. Migr. *7*, 27-32.

Smet, W., Sevilem, I., de Luis Balaguer, M.A., Wybouw, B., Mor, E., Miyashima, S., Blob, B., Roszak, P., Jacobs, T.B., Boekschoten, M., et al. (2019). DOF2. 1 controls cytokinin-dependent vascular cell proliferation downstream of TMO5/LHW. Curr. Biol. *29*, 520-529.e6.

Smetana, O., Makila, R., Lyu, M., Amiryousefi, A., Rodriguez, F.S., Wu, M.F., Sole-Gil, A., Gavarron, M.L., Siligato, R., Miyashima, S., et al. (2019). High levels of auxin signalling define the stem-cell organizer of the vascular cambium. Nature *565*, 485-489.

Stadler, R. and Sauer, N. (1996). The Arabidopsis thaliana AtSUC2 gene is specifically expressed in companion cells. Bot. Acta *109*, 299-306.

Wendrich, J.R., Moller, B.K., Li, S., Saiga, S., Sozzani, R., Benfey, P.N., De Rybel, B., and Weijers, D. (2017). Framework for gradual progression of cell ontogeny in the Arabidopsis root meristem. Proc. Natl. Acad. Sci. U. S. A. *114*, E8922-E8929.

Yamaguchi, Y. and Huffaker, A. (2011). Endogenous peptide elicitors in higher plants. Curr. Opin. Plant Biol. *14*, 351-357.

Yamaguchi, Y., Huffaker, A., Bryan, A.C., Tax, F.E., and Ryan, C.A. (2010). PEPR2 is a second receptor for the Pep1 and Pep2 peptides and contributes to defense responses in Arabidopsis. Plant Cell *22*, 508-522.

Ye, L., Wang, X., Lyu, M., Siligato, R., Eswaran, G., Vainio, L., Blomster, T., Zhang, J., and Mähönen, A.P. (2021). Cytokinins initiate secondary growth in the Arabidopsis root through a set of LBD genes. Curr. Biol. *31*, 3365-3373.e7.

Zhang, J., Eswaran, G., Alonso-Serra, J., Kucukoglu, M., Xiang, J., Yang, W., Elo, A., Nieminen, K., Damén, T., Joung, J.G., et al. (2019). Transcriptional regulatory framework for vascular cambium development in Arabidopsis roots. Nat. Plants *5*, 1033-1042.

Zhou, F., Emonet, A., Tendon, V.D., Marhavy, P., Wu, D., Lahaye, T., and Geldner, N. (2020). Co-incidence of damage and microbial patterns controls localized immune responses in roots. Cell *180*, 440-453.e18.

Zhou, J., Wang, X., Lee, J.Y., and Lee, J.Y. (2013). Cell-to-cell movement of two interacting AT-hook factors in Arabidopsis root vascular tissue patterning. Plant Cell *25*, 187-201.

Zipfel, C., Robatzek, S., Navarro, L., Oakeley, E.J., Jones, J.D.G., Felix, G., and Boller, T. (2004). Bacterial disease resistance in Arabidopsis through flagellin perception. Nature *428*, 764-767.